Deep Learning and Optimization Algorithms Based PV Power Forecast for an Effective Hybrid System Energy Management

Rim Ben Ammar*‡, Mohsen Ben Ammar**, Abdelmajid Oualha*

*LETI Laboratory, ENIS, (National Engineering School of Sfax), University of Sfax, Tunisia

**CEM Laboratory, ENIS, University of Sfax, Tunisia

(rim.benammar@enis.tn, mohsen.benammar@enis.tn, abdelmajid.oualha@enis.tn)

‡ Corresponding Author; Rim Ben Ammar, ENIS, University of Sfax, Tunisia,

Tél: +216 70 258 520, Fax: +216 74 275 595, rim.benammar@enis.tn

Received: 30.11.2021 Accepted: 08.01.2022

Abstract- Economic and demographic development has led to energy consumption increment around the world. The utilization of renewable energies is the best solution to offset this increase. The photovoltaic energy is widely used around the word through grid connection or standalone systems. Climatic changes can influence the generated power and the operating management strategy. Thus, photovoltaic power forecasting is very crucial to ensure stability. Reliable prediction accuracy provides information to ensure an efficient energy management of a PV/Battery/Diesel hybrid system. This paper presents a comparative study among various photovoltaic power prediction methods based on deep learning and optimization algorithms. Three topologies are outlined: the feed forward neural network with Particle- Swarm-Optimization tool (FFNN-PSO), the long short-term memory recurrent neural network (LSTM) and the bidirectional LSTM network with the Bayesian Optimization Algorithm (BiLSTM-BOA). The predictors' accuracy evaluation is done via statistical metrics. The simulation analysis show the performance of the BiLSTM-BOA on photovoltaic power forecasting. The application of the management algorithm using the forecasted PV power proved a high level of efficiency for both clear and disturb days. It maximizes the contribution of the renewable resource, minimizes the utilization of the batteries and the diesel generators and ensures load supply continuity.

Keywords Photovoltaic power, forecasting, deep learning, optimization, management.

Nomenclature

A_d: Battery daily autonomy [day]
C_B: Battery capacity [Ah]
C_T: Total batteries capacity [Ah]
dod_{max}: Battery maximum depth of discharge
$E_{batceln}$: Nominal amount of energy of one battery [Wh]
E_{batn}: Batteries nominal amount of energy [Wh]
E_L: The mean daily produced PV power [Wh/day]
E_{Batc}: Charged battery power [Wh]
E_{Batd}: Discharged battery power [Wh]
P_L: The load power [W]
$E_{Batcmax}$: The maximum battery charged power [Wh]
$E_{Batdmax}$: The maximum battery discharged power [Wh]
E_{socmin}: Batteries minimum amount of energy [Wh]
E_{socmax}: Batteries maximum amount of energy [Wh]
E_{soc}: Batteries amount of energy variation [Wh]
P_{DGn}: Diesel generator nominal power [W]
P_{DG}: Diesel generator power [W]
P_{dump}: The dumped power [W]
P_{PV}: The predicted photovoltaic power [W]

1. Introduction

Due to the excessive economic and demographic development, the utilization of the renewables energies has been increased all over the other sources [1-2]. Thanks to their advantages including property and durability [3]. The most utilized source is the photovoltaic energy [4]. The PV panel converts the sunlight into electrical energy. The intermittent character is the main drawbacks of the generated power [5]. It depends on the variable climatic data such as sun radiation and

temperature [6]. Indeed, the produced power can be more effective on a clear day than on a cloudy day. Thus, to maximize its contribution, an effective photovoltaic power-forecasting tool is mandatory [7-9]. The main predicted power is a helpful tool for energy managers to guarantee an optimal energy dispatch [10]. The photovoltaic power forecast methodologies could be divided on five categories: The persistence forecast is based on the theory that today equal to tomorrow defined with a mathematical equation [11-12]. The physical models, which impose the knowledge of the astronomical parameters [13-14]. The statistical methods based on a pure mathematical process e.g. the curve fitting, the autoregressive moving average model, the exponentially weighted moving average (EWMA) [15-16]. The deep learning techniques that enclose the feed forward neural network, the multilayer perceptron neural network and the recurrent neural network [17-19]. The hybrid models, which present a combination of two or more topologies. It takes the potential of all the combined techniques. For example, the ANFIS model that combine ANN and fuzzy logic, the ANN with the Wavelet Transform, the ANN with the support vector machine, the multilayer perceptron and grey wolf, ant lion and whale optimization algorithms [20-23]. The most accurate tools relies on deep learning networks including recurrent and non-recurrent structure. Moreover, they have been used in different tasks such as face recognition [24-25], wireless sensor network [26-27]. They can be combined with an optimization tools for more accurate prediction results [28-31]. In our paper, three types of artificial networks are proposed: the feed forward neural network with Particle-Swarm-Optimization tool (FFNN-PSO), the long short-term memory recurrent neural network (LSTM) and the bidirectional LSTM network with the Bayesian Optimization Algorithm (BiLSTM-BOA). The mentioned methods performances have been compared via statistical metrics. The simulation results show that the BiLSTM-BOA topology is the most accurate. It encloses the benefits of the BiLSTM network, as it performs the training on both the forward and the backward path, and the BOA, as it performs an effective optimization of the BiLSTM hyperparameters. As application of the forecasted PV power, the energy management of a hybrid system. The studied system consists of a PV station, bidirectional inverter, batteries and diesel generators. The management strategy respects the following criteria: maximization of the renewable source utilization, minimization of the batteries and the diesel generators use, protection of the storage systems from over-charging or discharging and load-supply continuity. The simulation results for both clear and disturb days show a full respect of the designed criteria. The main process is summarized on the flowchart presented in figure 1.

The main contributions of this study can be presented as follows: (a) An advanced PV power prediction models based on deep learning and optimization algorithms are proposed (b) Accuracy prediction levels are compared based on the performance evaluation metrics and the training time, for both stable and disturb days (c) Exploitation of the forecasted PV power on a hybrid PV/Battery/Diesel energy management. The main study presents a useful reference on the combination between the optimization algorithms and the deep learning networks for the generated PV power forecast.

The following paper is organized as follow: section 3 describes the proposed methods, section 4 summarizes the statistical metrics, section 5 presents the hybrid system components description and the proposed management algorithm, section 6 displays the simulation results and section 7 outlines the conclusion.

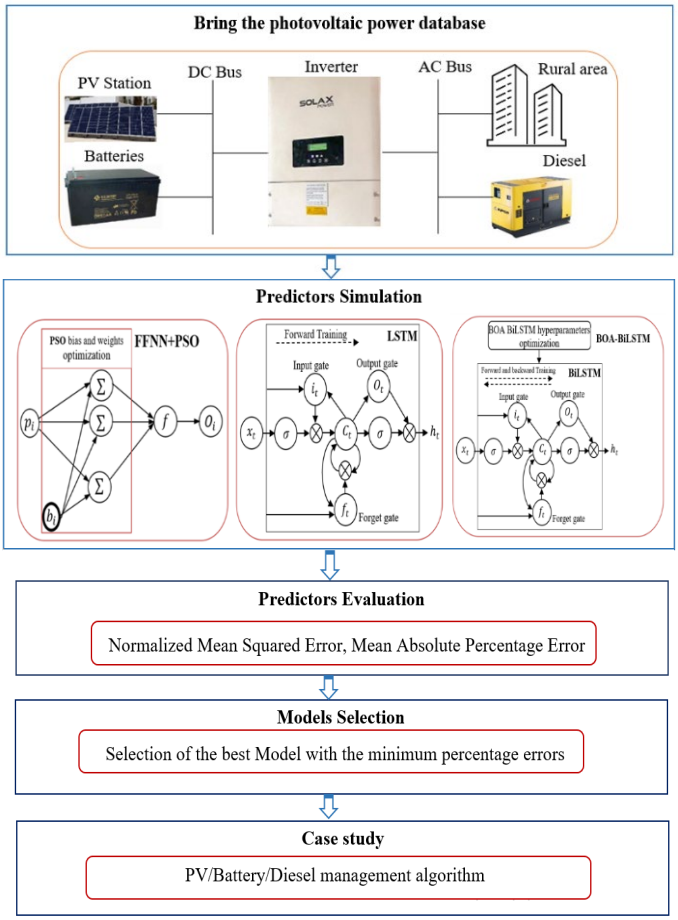

Fig. 1. Methodology of the proposed approach.

2. Methodologies description

For PV power production forecasting, three topologies based on deep learning and optimization algorithms have been considered. We have used different architectures: the feed forward neural network with Particle- Swarm-Optimization tool (FFNN-PSO), the long short-term memory recurrent neural network (LSTM) and the bidirectional LSTM network with the Bayesian Optimization Algorithm (BiLSTM-BOA). Below, a brief description of each topology.

2.1. Feed Forward algorithm-Particle Swarm Optimization (FFNN-PSO)

The FFNN information flow is done in one direction from the input to the output layer [32]. The FFNN output with a linear function can be expressed as follow [33].

$$O_j = f\left(\sum_{i=1}^{n} \omega_{ij} p_i + b_j\right) \quad (1)$$

Where, f is the sigmoid hidden layer's activation function, p_i is the input data, ω_{ij} are the weights between the input and the hidden layers and b_j presents the bias value of neuron j of the hidden layer. Linear activation function was chosen for the output layer.

The FFNN involves two primordial steps, which are training and validation. During the learning process, the bias and the weights parameters are updated to meet the desired output value based on the back propagation. The main process can be fell down on local minima [34]. To solve this problem, the cited factors should be updated with another technique such as the particle-swarm-optimization-algorithm. It is characterized with its faster and greater training results [35-36]. The PSO, invented by Russell Eberhart and James Kennedy, consists of a population optimization tool inspired from birds flocking around food sources [37-39]. Indeed, the PSO is initialized with a random particles population. The main algorithm process focuses on optima through generations update. All the particles present fitness values, which are evaluated based on a fitness function [40]. The mean squared error was defined as a fitness function. It can be calculated using equation (2).

$$MSE = \frac{\sum_{i=1}^{n}(O_i - O_{iD})^2}{n} \quad (2)$$

Where, O_i is the network's output, $O_{iD}$is the desired output and n: is the total number of data.

Each particle is characterized with its specific position and velocity, which are updated using equations (3) [41].

$$s_{k+1}^i = s_k^i + v_{k+1}^i \quad (3)$$

Where:

s_{k+1}^i: Particle i position at time instant $k+1$

s_k^i : Particle i position at time instant k

v_{k+1}^i: Particle i velocity at time instant $k+1$

v_k^i: Particle i velocity at time instant k

ω_k: The inertia weight

$c_1; c_2$: The acceleration constants

$r_1; r_2$: Random elements

φ_k^i: The best solution reached by the designed particle

φ_k^g: The best solution reached by the entire particles

The FFNN+PSO optimization algorithm can be summarized on the following organogram presented in figure 2.

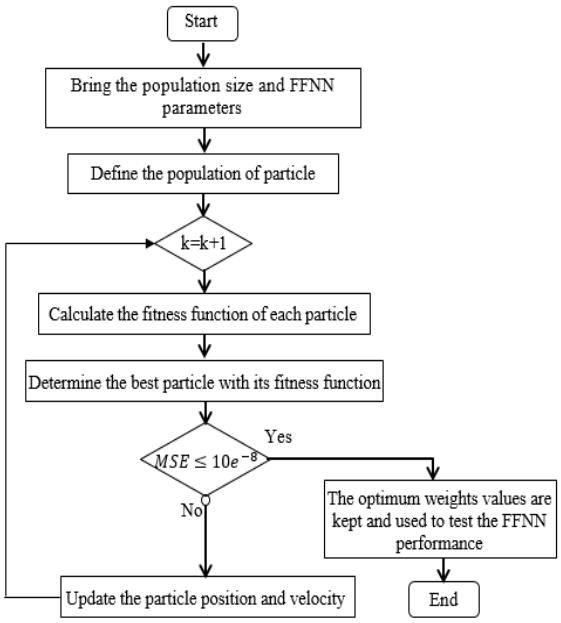

Fig. 2. FFNN-PSO flowchart.

2.2. Long Short-Term Memory (LSTM)

LSTM is a subtype of recurrent neural network. LSTM and RNN consist of internal self-looped repeating networks. The difference between them is the repeating module structure. Indeed, the RNN involves a simple repeating model based on a simple layer such us 'Tanh layer'. However, the LSTM presents four layers including the 'Tanh layer' [42]. The LSTM utilizes the hidden layer unit, namely memory cells, to overcome the RNN limitation. Three gates are designed for memory cells control, which are the input gate, the output gate, and the forget gate. The memory flow control is done through the input and the output gates. The forget gate is added to the memory cell that straight the output information with weights update from previous to next neuron[43-44].

The forget gate output derives the information that should be forget from the previous step. It can be expressed using equation (4).

$$f_t = \sigma\left(W_f \cdot [h_{t-1}, x_t] + b_f\right) \quad (4)$$

The input gate derives the information that should be stored in the cell state. It can be displayed using equation (5).

$$i_t = \sigma(W_i \cdot [h_{t-1}, x_t] + b_i) \quad (5)$$

The third layer is the 'Tanh layer'. It can be used to generate new values that can be added to the state. It can be expressed using equation (6).

$$\widetilde{C_t} = \varphi(W_C \cdot [h_{t-1}, x_t] + b_C) \quad (6)$$

After the application of the cited three layers, the previous cell state C_{t-1} should be updated, the forget gate derives what should be forgotten, the input gate derives what should be added to the new cell state $\widetilde{C_t}$. The cell state update can be formulated using equation (7).

$$C_t = f_t C_{t-1} + i_t \widetilde{C_t} \quad (7)$$

The output gate derives the output of the whole process, after the cell update. The final output can be expressed using equation (8).

$$O_t = \sigma(W_O \cdot [h_{t-1}, x_t] + b_O) \cdot \varphi(C_t) \quad (8)$$

Where: $(W_f, W_i, W_C, W_O)$are the weights of each layer, (b_f, b_i, b_C, b_O) are the bias of each layer, σ denotes the sigmoid activation function and φ is the Tanh function.

The LSTM loss function is the mean squared function between the output of the LSTM topology and the truth data. It can be formulated as follow using equation (9).

$$Loss(\theta)_{LSTM} = \frac{1}{N}\sum_{i=1}^{N}|NN(x_i;\theta) - y_i|^2 \quad (9)$$

Where: $\theta = \{W, b\}$; $W = [W_f, W_i, W_C, W_O]$, $b = [b_f, b_i, b_C, b_O]$; N is the number of data

The loss function minimization can be done through stochastic gradient descent algorithm.

2.3. The Bayesian optimization algorithm (BOA)

The Bayesian optimization algorithm is used to pick out the hyperparameters optimal values with fewer iterations. The main idea of BOA is to suppose a prior distribution model of f (X) at first, after that utilize the derived information for guess model optimization in accordance with the actual distribution. Thus, the BOA selects the parameters for results improvement. It maximizes the global optimum via the previous sampling point information [45].

The steps of the BOA are as follows [46]: First, suppose a prior function. Commonly, the Gaussian Processes (GP) is utilized as the assumed model. Then, involve two input sets of real data $[X_0, f(X_0)], [X_1, f(X_1)]$into the GP model to rectify the assumed model. After that, select a set X_i from the rectified GP. The designated criterion requires the ability of the selected set to improve the acquisition function. Finally, the $f(X_i)$ value is calculated. If the iteration number fulfill the whole dataset, the results are generated. If not, an input $[X_i, f(X_i)]$ is implanted on the GP, re-rectify the model and repeat the followed steps until dealing with all the sets.

The BOA is utilized for the bidirectional LSTM model (BiLSTM) parameters optimization. The main difference between LSTM and the BiLSTM lies on the training process. Indeed, the LSTM train the data only on one direction. However, the BiLSTM train the data on the forward and the backward path [47] as presented in figure 3.

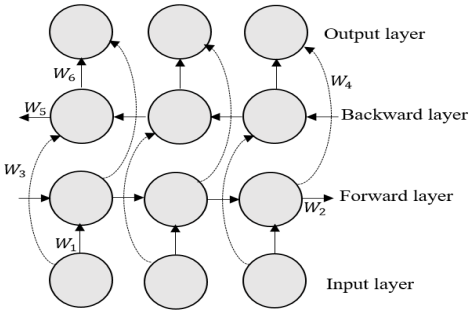

Fig. 3. BiLSTM structure.

The BiLSTM model forward, backward and output layers expressions can be expressed using equations (10), (11) and (12), respectively [48].

$$\vec{h}_t = H\left(W_1 x_t + W_2 \vec{h}_{t-1} + \vec{b}\right) \quad (10)$$

$$\overleftarrow{h}_t = H\left(W_3 x_t + W_5 \overleftarrow{h}_{t-1} + \overleftarrow{b}\right) \quad (11)$$

$$y_t = W_4 \vec{h}_t + W_6 \overleftarrow{h}_t + b_y \quad (12)$$

Where: W_1, W_2, W_3, W_4, W_5, W_6 are de corresponding weights, $\vec{b}$, $\overleftarrow{b}$, b_y are the forward, backward and the output biases.

3. Statistical evaluation metrics

The evaluation of the proposed technologies can be done through statistical metrics such us: the normalized mean squared error, the mean absolute percentage error and the normalized error. The cited measures compare between the real and the predicted data to assimilate the performance of the utilized model [49-51]. The following metrics can be expressed using equations (13), (14) and (15).

The Normalized root mean squared error:

$$NRMSE(\%) = 100 \times \left(\sqrt{\frac{1}{N}\sum_{i=1}^{N}\left(P_i - \hat{P}_i\right)^2} \Big/ \frac{1}{N}\sum_{i=1}^{N} P_i\right) \quad (13)$$

The mean absolute percentage error:

$$MAPE(\%) = 100 \cdot \left(\frac{1}{N}\sum_{i=1}^{N}\left|\frac{P_i - \hat{P}_i}{P_i}\right|\right) \quad (14)$$

The normalized error:

$$NE = \frac{|P_i - \hat{P}_i|}{\max(P_i)} \quad (15)$$

Where: P_i is the real value, $\hat{P}_i$ is the predicted value and N is the observations number.

4. Hybrid PV/Battery/Diesel system management

Standalone hybrid systems are widely used in remote area where there is not access to the power grid [52-53]. In our paper, the hybrid system main components are the PV generator, the batteries, the bidirectional inverter and the diesel generator. The load is supplied mostly through the renewable source and the batteries and the diesel generator intervene only when there is lack of energy. The PV generator model, the batteries storage system, the diesel generator and the energy management algorithm are discussed as follow.

4.1. PV generator modelling

The generated PV Power can be calculated considering the solar irradiation and the ambient temperature meteorological parameters [54-55]. The mathematical model of the produced energy can be expressed as follow in equation (16) [56].

$$P_{PV}(t) = N_{PV} P_{PV_{STC}} \frac{SR(t)}{SR_{STC}}\left(1 + \frac{\alpha_P}{100}(T_{cell}(t) - T_{STC})\right) f_{PV} \quad (16)$$

Where: N_{PV} is the number of the photovoltaic panels, $P_{PV_{STC}}$ is the photovoltaic power rate on the nominal condition

STC ($SR_{STC} = 1000W/m^2, T_{STC} = 25℃, AM = 1.5$), $SR(t)$ is the solar irradiation at time t, α_P is the temperature coefficient of maximum power, $T_{cell}(t)$ is the cell temperature at time t and f_{PV} is the derating factor that consider the losses due to shading and natural degradation of the PV Panel.

The cell temperature can be calculated using equation (17).

$$T_{cell}(t) = T_{amb}(t) + SR(t)\left(\frac{NOCT-25}{1000}\right) \quad (17)$$

Where $T_{amb}(t)$ is the ambient temperature at time t and NOCT is the nominal operating cell temperature.

4.2. Battery modelling

Standalone photovoltaic system requires storage components. The most used are the batteries due to their efficiency and their cheaper cost [57]. The battery bank is characterized with its state of charge and the terminal voltage [58].

The total capacity of the battery bank to meet the load can be calculated using equation (18) [59].

$$C_T = \frac{E_L A_d}{U_T\, dod_{max}} \quad (18)$$

Where: E_L is the mean daily produced PV power, A_d is the battery autonomy, dod_{max} is the battery maximum depth of discharge, U_T is he voltage related to how much batteries are installed in series.

The number of batteries in parallel can be deducted through the following equation (19).

$$N_{bP} = \frac{C_T}{C_B} \quad (19)$$

Where: C_B is the capacity of one battery.

The battery bank nominal amount of energy can be expressed using equation (20).

$$E_{Batn} = N_{bP} N_{bS} E_{batcelln} \quad (20)$$

Where: N_{bP} is the number of batteries in parallel, N_{bS} is the number of batteries in series and $E_{batcelln}$ is the nominal capacity of one battery, which is the product of the battery capacity and voltage.

The battery bank amount of energy depends on the required load power and the generated energy. Its variation during the charging and the discharging process can be expressed using equations (21) and (22) as follow.

During the charging process:

$$E_{soc}(t+1) = E_{soc}(t)(1-\sigma_B) + E_{Batc}(t)\eta_{Batc} \quad (21)$$

During the discharging process:

$$E_{soc}(t+1) = E_{soc}(t)(1-\sigma_B) - E_{Batd}(t)\eta_{Batd} \quad (22)$$

Where: $E_{soc}(t)$ is the batteries' amount of energy at time (t), σ_B is the battery self-discharge parameter, $E_{Batc}(t)$ is the designed energy to charge the batteries, $E_{Batd}(t)$ is the discharged energy to feed the load requirements, generated power at time t and η_{Batc}, η_{Batd} are the battery efficiency during the charging and the discharging processes comprised between 0 and 1, respectively.

The battery can be charged or discharged in coordination with a specific quantity of energy. The maximum energies can be defined using equations (23) and (24).

$$E_{Batcmax} = E_{socmax} - E_{soc}(t) \quad (23)$$

$$E_{Batdmax} = E_{soc}(t) - E_{socmin} \quad (24)$$

The battery bank amount of energy should be limited between minimum and maximum values to avoid overcharging and discharging issues. The minimum and the maximum amount of energy values can determined based on equations (25) and (26), respectively.

$$E_{socmin} = (1 - dod_{max})E_{Batn} \quad (25)$$

$$E_{socmax} = E_{Batn} \quad (26)$$

4.3. Diesel generator modelling

The dispatch strategy involved in our paper consists on running the diesel generator (DG) only when the generated photovoltaic power and the stored energy on the batteries are not sufficient to meet the load requirements [60].

The number of DG units required to ensure Power-Load equilibrium can be expressed using equation (27).

$$NDG_{ON}(t) = \min\left(N_{DGMAX}, round\left(\frac{P_{DG}(t)}{P_{DGn}}\right)\right) \quad (27)$$

4.4. Energy management algorithm

The PV/Battery/Diesel energy management algorithm (EMA) considers the renewable resource as the first load supplier, the battery bank is only charged through the generated PV Power and the diesel generator is only required when the produced energy through the PV generator and the stored energy on the batteries are not sufficient to meet the load demand. The EMA aims to maximize the use of the renewable source, minimize the utilization of the batteries and the diesel generators, protect the storage systems for over charging or discharging and ensure the continuity of the load supply.

The following cases describe the management strategy used in our paper. The first case is when the generated PV power is equal to the load requirements. The load is supplied through the renewable source, there is no excess energy stored in the batteries and the DG is off.

The second case is when the produced PV power is higher than the load demand. The load is supplied through the PV station. The excess of energy is used to charge the batteries. If the batteries are fully charged, this energy is dumped. In this case, the DG also is off.

The third case is when the produced PV power is lower than the load demand. The load is supplied through the PV station and the batteries, if there is sufficient energy. If not the diesel, generator is turning on. In this case, the PV generator charges the battery bank with the needed energy depending on

its capacity and the load requirements are covered using the DG and the rest of the PV power.

The last case is when there is no energy from the PV generator. The load is supplied through the DG and the batteries.

The mentioned strategies can be summarized on the following flowchart presented in figure 4.

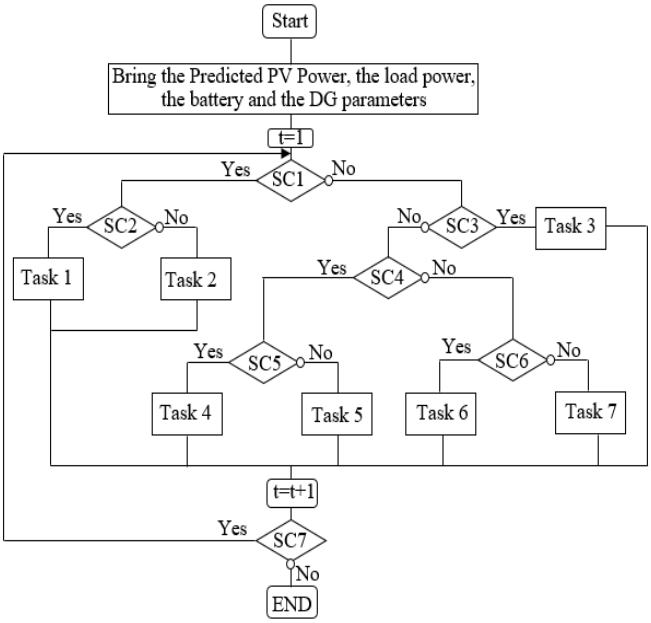

Fig. 4. Hybrid PV/Battery/Diesel management algorithm.

The mentioned tasks and conditions presented in the designed management algorithm below can be described through mathematical equations in table 1.

Table 1. Management algorithm tasks and conditions equations.

SC1	$P_L(t) - P_{PV}(t)\eta_{inv} \leq 0$
SC2	$P_L(t) - P_{PV}(t)\eta_{inv} \leq E_{Batcmax}(t)\,\eta_{inv}$
Task 1	$E_{Batc}(t) = P_{PV}(t) - P_L(t)/\eta_{inv})$ $E_{soc}(t+1) = E_{soc}(t)(1-\sigma_B) + E_{Batc}(t)\eta_{Batc}$; $P_{Dump}(t) = 0$
Task 2	$E_{Batc}(t) = E_{Batcmax}(t)$; $E_{soc}(t+1) =$ $E_{soc}(t)(1-\sigma_B) + E_{Batc}(t)\eta_{Batc}$ $P_{Dump}(t) = 0$
SC3	$P_L(t) - P_{PV}(t)\eta_{inv} \leq E_{Batdmax}(t)\,\eta_{inv}$
Task 3	$E_{Batd}(t) = P_L(t)/\eta_{inv} - P_{PV}(t)$ $E_{soc}(t+1) = E_{soc}(t)(1-\sigma_B) - E_{Batd}(t)\eta_{Batd}$
SC4	$P_{PV}(t) > 0$
SC5	$P_{PV}(t) \geq E_{Batcmax}(t)$
Task 4	$E_{Batc}(t) = E_{Batcmax}(t)$ $E_{soc}(t+1) =$ $E_{soc}(t)(1-\sigma_B) + E_{Batc}(t)\eta_{Batc}$ $P_{DG}(t) = P_L(t) - \big(P_{PV}(t) - E_{Batc}(t)\big)\eta_{inv})$; $P_{Dump}(t) = 0$ $N_{DGON}(t) = round(P_{DG}(t)/P_{DGn}$
Task 5	$E_{Batc}(t) = P_{PV}(t)$; $E_{soc}(t+1) = E_{soc}(t)(1-$ $\sigma_B) + E_{Batc}(t)\eta_{Batc}$ $P_{DG}(t) = P_L(t)$; $N_{DGON}(t) =$ $round(P_{DG}(t)/P_{DGn}$; $P_{Dump}(t) = 0$
SC6	$P_L(t) - E_{Batdmax}\,(t)\eta_{inv} \geq P_{DGn}$
Task 6	$E_{Batd}(t) = E_{Batdmax}(t)$; $E_{soc}(t+1) =$ $E_{soc}(t)(1-\sigma_B) - E_{Batd}(t)\eta_{Batd}$ $P_{DG}(t) = P_L(t) - E_{Batd}(t)\eta_{inv})$; $N_{DGON}(t) =$ $round(P_{DG}(t)/P_{DGn}$ $P_{Dump}(t) = 0$; $E_{Batc}(t) = 0$
Task 7	$N_{DGON}(t) = 1$ $P_{DG}(t) = P_{DGn}$; $E_{Batd}(t) =$ $\big(P_L(t) - P_{DG}(t)\big)/\eta_{inv}$ $E_{soc}(t+1) = E_{soc}(t)(1-\sigma_B) - E_{Batd}(t)\eta_{Batd}$ $P_{Dump}(t) = 0$; $E_{Batc}(t) = 0$
SC7	$P_L(t) > 0$

5. Simulation and Results

5.1. Photovoltaic Power prediction results

The utilized database encloses the photovoltaic power for clear and disturb days. For the first category, the training data are spread out from 20 July to 28 July 2017 and the testing data allied to 29 July 2017. For the disturb day, the training data are expanded from 20 December to 28 December 2017 and the testing date unfold 29 December 2017. Three methods were simulated for both mentioned days: the FFNN-PSO, the LSTM and the BiLSTM-BOA.

5.1.1. FFNN-PSO best topology selection

The FFNN requires the determination of the optimum number of neurons in the hidden layer. Thus, a trial and error method was involved to find out the best neural network architecture with the minimum errors. The simulation results provide the perfect topologies, 2 neurons in the hidden layer for the clear day and 4 neurons in the hidden layers for the disturb day. The PSO algorithm intervenes on the determination of the FFNN optimized synaptic weights and biases.

The PSO parameters are depicted in table 2.

Table 2. The PSO parameters.

Parameter	Value
Maximum number of iterations	250
Population size	100
Inertia weight	1
Inertia weight damping ratio	0.99
Acceleration coefficient C_1	1.5
Acceleration coefficient C_2	2
Test Function	MSE

5.1.2. LSTM topology selection

The application of the LSTM was done through MATLAB. The first step consists on the determination of the training and the test datasets. The second step focuses on data standardization to ensure a zero mean and a unit variance. This step restrains the LSTM from overfitting. The third step focuses on the determination of the LSTM network structure, which encloses four layer: the sequence input layer, the LSTM layer characterized with a sigmoid gate, a Tanh state activation functions and 200 hidden units, the fully connected layer and the regression output layer. The fourth step displays the training options as presented in table 3. Finally, the training, validation and test of the designed network.

Table 3. The training options parameters.

Parameter	Value
Gradient decay factor	0.9
Epsilon	1e-08
Initial learn rate	0.005
Learn rate schedule	piecewise
Learn rate drop factor	0.2
Learn rate drop period	125
Gradient threshold	1
Max epochs	250
Mini batch size	128

The training process of the LSTM model encloses the RMSE and the loss function variation during the training and the validation processes.

5.1.3. BiLSTM-BOA topology selection

The Bayesian optimization was used for the BiLSTM hyperparameters selection. The BOA focuses on the following hyperparameters: the number of neurons, the learning rate and the L2Regularization. The low number of neurons may not achieves high level of accuracy; the large value may affects the model performance. The large value of the learning rate engenders a rapid convergence without dealing with the optimum network; the low value enables the network to converge at a specific simulation time. The L²Regularization optimized value restrains the model from overfitting. The hyperparameters optimized values are presented in table 4 for both clear and disturb days.

Table 4. The BiLSTM hyperparameters.

Hyperparameter	Clear day	Disturb day
Number of neurons	78	189
Initial learning rate	0.013386	0.040658
L²Regularization	1.3388e-10	2.4442e-10

5.1.4. Models performances evaluation

The selected models were tested for two types of days: clear and disturb days. The simulation results of the predicted photovoltaic power and the designed normalized error for the clear and the disturb days are presented in figures 5 and 6.

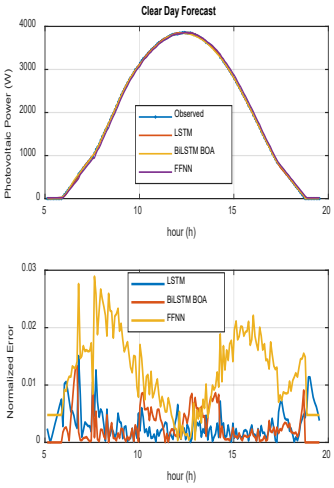

Fig. 5.Clear day PV power forecast.

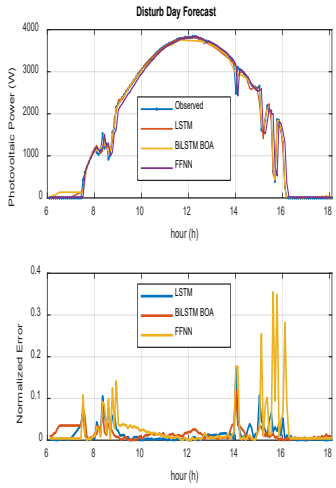

Fig. 6. Disturb day PV power forecast.

The evaluation of the topologies accuracy on PV power forecasting, was tested through the statistical metrics as presented in table 5. The percentage errors show that the BiLSTM-BOA is the most accurate model with an NRMSE and a MAPE values equal to 0.74% and 1.84% for the clear day and 4.39% and 5.24% for the cloudy day. the LSTM model shows an effective prediction accuracy for the different days with a NRMSE and a MAPE equal to 0.81% and 2.12% for the clear day and 5.47%and 8.45% for the disturb day. However the FFNN-PSO topology is mostly recommended for a clear day rather than a disturb day. The FFNN-PSO accuracy evaluators for the clear day are lower than those of the disturb day and does not exceed 6.37%. Above the following results, we can conclude that the LSTM and the BiLSTM-BOA can accurately fit the PV Power for different climatic conditions, the FFNN-PSO model performs better for a clear day without fluctuations and the BiLSTM-BOA ensures predictions with high precision level. The impressive results derived with the BiLSTM-BOA predictors is based on the training process of the forward and the backward path and the effective choice of the hyperparameters using the Bayesian optimization.

Table 5. Models accuracy evaluation.

	Clear day		*Disturb day*	
	NRMSE (%)	MAPE (%)	NRMSE (%)	MAPE (%)
FFNN-PSO	2.67	6.37	12.74	43.86
LSTM	0.81	2.12	5.47	8.45
BiLSTM-BOA	0.74	1.84	4.39	5.24

The training time is an important parameter for accuracy model determination. The simulation time of the proposed models are displayed in table 6. The BiLSTM-BOA model ensures an accurate prediction results, on the other hand it demands more training time comparing with the other cited topologies. The training time is in the range of 69944.1062 seconds for the disturb day and 36336.015 for the clear day. The LSTM algorithm presents the lowest training time, it is equal to 672.47 seconds for the clear day and 684.1062 seconds for the disturb day.

Table 6. Models training time evaluation.

	Training time (s)	
	Clear day	*Disturb day*
FFNN-PSO	1005.379	1044.445
LSTM	672.470	684.534
BiLSTM-BOA	36336.015	69944.1062

5.2. Case study using the forecasted photovoltaic power

The studied hybrid installation encloses photovoltaic station, batteries diesel generators and a bidirectional inverter. The main objective consists on the flow energy management using as input data the forecasted PV power, the load and the electrical parameters of the cited components. The technical parameters are defined in table 7.

Table 7. Components technical parameters.

Component	**Technical parameter**	**Value**
PV Sun module Pro series SW-250	Maximum power [Wp]	250
	Open circuit voltage [V]	37.6
	Maximum power point voltage, [V]	30.5
	Short circuit current [A]	8.81
	Maximum power point current [A]	8.27
	Power temperature coefficient α_P [%/K]	-0.45
	Nominal operating cell temperature [°C]	46
	Derating Factor	0.85
	Number of PV panels	16
	Nominal Voltage [V]	12
Battery VRLA BPL 210-12	Nominal Capacity [Ah]	210
	DC system voltage [V]	24
	Capacity Rate [h]	20
	Charge efficiency	0.98
	discharge efficiency	1
	Self-discharge rate	0.000083
	Maximum Depth of Discharge	0.89
	Battery daily autonomy [day]	3
	Number of batteries	36
Diesel generator	Nominal diesel generator power [W]	500
	Number of diesel generators	5
Bidirectioanl Inverter	Inverter efficiency	0.99

The Predicted PV and the designed load, related for both clear and disturb days, are presented in figures 7 and 8.

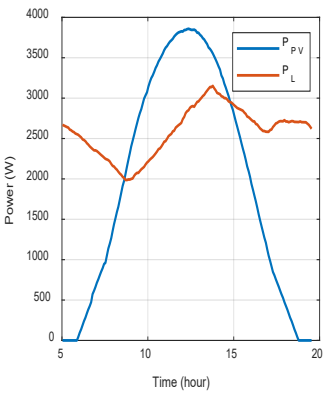

Fig. 7. PV-Load Clear day.

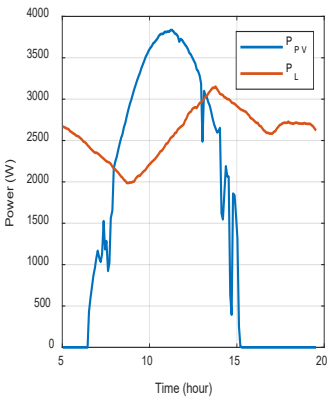

Fig. 8. PV-Load Disturb day.

The Application of the management algorithm cited below, for the clear day, using Matlab M-File gives the following results presented in figures 9 and 10.

Figure 9 presents the power contribution of the PV panel, the batteries power during charging and discharging processes and the diesel generator energy in coordination with the number of DG turning ON to provide the load power demand. 5 or 2 diesels are turning ON depending on the required power.

As shown in figure 10, the load requirements are covered through the PV station with a percentage value equal to 32%, the batteries contribution is 15% and finally the diesel generator presents the minor percentage in the order of 3%. The main results confirm the management algorithm criteria basically the maximization of the renewable source contribution and the minimization of the DG utilization.

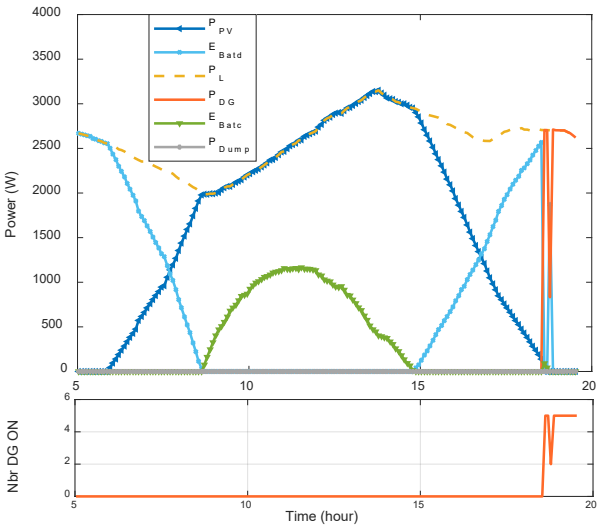

Fig. 9. PV/Battery/Diesel energy management results (Clear day).

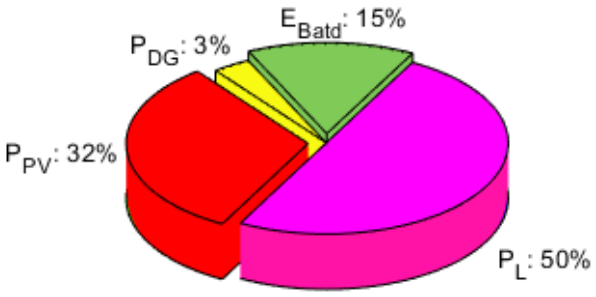

Fig. 10. PV/Battery/Diesel contribution percentages (Clear day).

The simulation results of the disturb day derived through the management algorithm application are presented in figures 11 and 12. Figure 11 presents the powers derived from the PV station, batteries and the diesel generator. 5 DG are turning ON to ensure the required load power. As shown in figure 12, the PV station contribution is in the range of 24%, the batteries contribution is equal to 15% and the DG contribution is in the order of 11%. The simulation results are in coordination with the EMA aims.

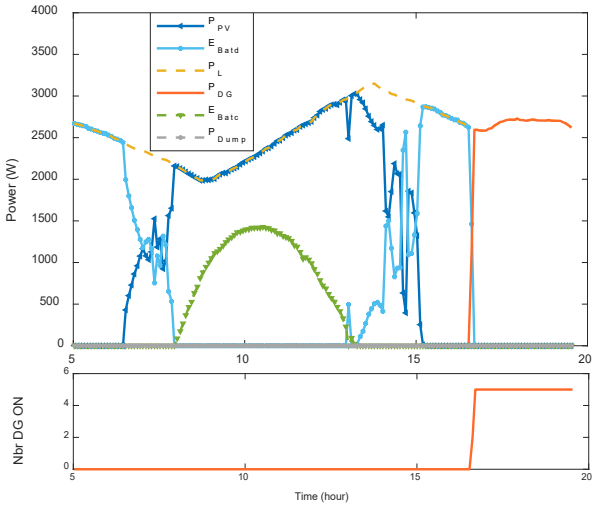

Fig. 11. PV/Battery/Diesel energy management results (Disturb day).

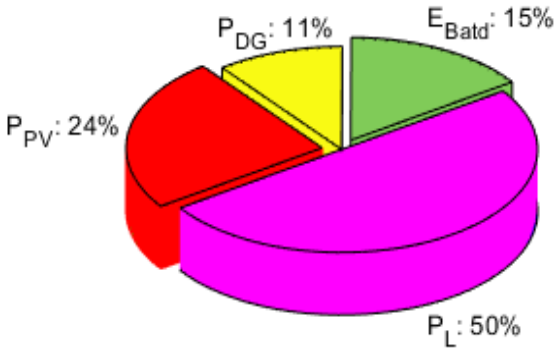

Fig. 12. PV/Battery/Diesel contribution percentages (Disturb day).

6. Conclusion

Photovoltaic power forecasting is an important task due to its fluctuation. Three predictors were proposed FFNN-PSO, LSTM and BiLSTM-BOA for both clear and disturb days. A comparative study between the mentioned methodologies was done through the designed curves and the statistical metrics. For the clear day, the simulation results show that all the topologies give satisfactory results as the accuracy evaluators does not exceed 6.37%. For the disturb day, LSTM and BiLSTM-BOA networks are more effective than the FFNN-PSO model. The NRMSE and the MAPE values does not surpass 8.45%. However, the BiLSTM-BOA structure ensures the most accurate prediction results for both clear and disturb days. It encloses the benefits of the BiLSTM network, as it performs the training on both the forward and the backward path, and the BOA, as it performs an effective optimization of the LSTM hyperparameters. The NRMSE and the MAPE percentages are equal to 0.74% and 1.84% for the clear day. For the cloudy day, they are in the range of 4.39% and 5.24%, respectively.

The predicted photovoltaic energy presents a promoted solution for rural areas, where there is not grid connection. The renewable resource should be coupled with storage systems and diesel generators to guarantee the continuity of load supply. Thus, an energy management algorithm was proposed. The designed algorithm ensures a maximum use of the PV power, a minimum use of the batteries and the diesel generators, continuity of service and storage systems protection. The main objectives were respected as shown in the simulation results done via the designed management strategy.

The advanced PV power prediction models based on deep learning and optimization algorithms show their accuracy on PV Power forecasting for different climatic conditions, mainly the BiLSTM-BOA Predictor. The forecasted energy is very important for an effective energy management strategy. As future work, the designed predictors can be applied for wind speed forecasting. The management strategy can be applied for hybrid system with two renewable sources of energy (PV/Wind), batteries and diesel generators.

References

[1] A. Ndiaye, M. A. Tankari and G. Lefebvre.: 'Adaptive neuro-fuzzy inference system application for the identification of a photovoltaic system and the forecasting of its maximum power point', In 2018 7th International Conference on Renewable Energy Research and Applications (ICRERA), IEEE, pp. 1061-1067, 2018.

[2] M. Yesilbudak, M. Çolak and R. Bayindir.: 'A review of data mining and solar power prediction. In 2016 IEEE International Conference on Renewable Energy Research and Applications (ICRERA), IEEE, pp. 1117-1121, 2016.

[3] L. Qi, M. Jiang, Y. Lv, Z. Zhang, J. Yan.: 'Techno-economic assessment of photovoltaic power generation mounted on cooling towers', Energy Conversion and Management, vol. 235, p. 113907, 2021.

[4] B. Dhivya, B and V. Prabu.: 'A Review of Renewable Energy Supply and Energy Efficiency Technologies', International Research Journal of Automotive Technology, vol. 1, No. 6, pp. 49-59, 2018.

[5] F. Ayadi, I. Colak, I. Garip and H. I. Bulbul.: 'Impacts of Renewable Energy Resources in Smart Grid. In 2020 8th International Conference on Smart Grid (icSmartGrid), IEEE, pp. 183-188, June 2020.

[6] W. Yuan, X. Wang, C. Su, C. Cheng, Z. Liu, and Z. Wu.: 'Stochastic optimization model for the short-term joint operation of photovoltaic power and hydropower plants based on chance-constrained programming', Energy, vol. 222, p. 119996, 2021.

[7] K.N. Nwaigwe, P. Mutabilwa and E. Dintwa, E.: 'An overview of solar power (PV systems) integration into electricity grids', Materials Science for Energy Technologies, vol. 2, No. 3, pp. 629-633, 2019.

[8] M. Yesilbudak, M. Colak and R. Bayindir.: 'What are the current status and future prospects in solar irradiance and solar power forecasting', International Journal of Renewable Energy Research (IJRER), Vol. 8, No.1, pp. 635-648, 2018.

[9] R. Bayindir, M. Yesilbudak, M. Colak and N. Genc.: 'A novel application of naive bayes classifier in photovoltaic energy prediction', In 2017 16th IEEE international conference on machine learning and applications (ICMLA), pp. 523-527, IEEE, December 2017.

[10] H. Zhen, D. Niu, K. Wang, Y. Shi, Y, Z. Ji and X. Xu, X.: 'Photovoltaic power forecasting based on GA improved Bi-LSTM in microgrid without meteorological information', Energy, vol. 231, p. 120908, 2021.

[11] J. Á. G. Ordiano, S. Waczowicz, M. Reischl, R. Mikut and V. Hagenmeyer.: 'Photovoltaic power forecasting using simple data-driven models without weather data', Computer Science-Research and Development, vol. 32, No. 1-2, pp. 237-246, 2017.

[12] G. Li, H. Wang, S. Zhang, J. Xin and H. Liu, H.: 'Recurrent neural networks based photovoltaic power forecasting approach', Energies, vol. 12, No. 13, p. 2538, 2019.

[13] R. B. Ammar, M.B. Ammar and A. Oualha.: 'Photovoltaic power forecast using empirical models and artificial intelligence approaches for water pumping systems', Renewable Energy, vol. 153, pp. 1016-1028, 2020.

[14] M.B. Ammar, R.B. Ammar and A. Oualha.: 'Photovoltaic power prediction for solar car park lighting office energy management', Journal of Energy Resources Technology, vol. 143, No. 3, pp. 1-11, 2021.

[15] A. Mindang and P. Siripongwutikorn, 'Solar Power Prediction in IoT Devices using Environmental and Location Factors', In Proceedings of the 2020 5th International Conference on Machine Learning Technologies, pp. 119-123, June 2020.

[16] H. Sharadga, S. Hajimirza and R.S. Balog.: 'Time series forecasting of solar power generation for large-scale photovoltaic plants', Renewable Energy, vol. 150, 7pp. 97-807, 2020.

[17] G. Perveen, M. Rizwan, N. Goel and P. Anand.: 'Artificial neural network models for global solar energy and photovoltaic power forecasting over India', Energy Sources Part A: Recovery, Utilization and Environmental Effects, vol. 2020, pp. 1-26, 2020.

[18] R.B. Ammar, M.B. Ammar and A. Oualha, A.: 'Comparative study among physical models and artificial intelligence methods for PV power forecasting', In 2021 18th International Multi-Conference on Systems, Signals & Devices (SSD), IEEE, pp. 1038-1046, March 2021.

[19] R.B. Ammar and A. Oualha.: 'Photovoltaic Power Prediction Using Recurrent Neural Networks', In: Derbel N., Zhu Q. (eds) Modeling, Identification and Control Methods in Renewable Energy Systems. Green Energy and Technology. Springer, Singapore, pp. 25-46, 2019.

[20] R.B. Ammar, M.B. Ammar and A. Oualha, A.: 'Photovoltaic power forecasting through temperature and solar radiation estimation', In 2019 16th International Multi-Conference on Systems, Signals & Devices (SSD), IEEE, pp. 691-699, March 2019.

[21] T. Zhang, C. Lv, F. Ma, K. Zhao, H. Wang and G.M. O'Hare.: 'A photovoltaic power forecasting model based on dendritic neuron networks with the aid of wavelet transform', Neurocomputing, vol. 397, pp. 438-446, 2020.

[22] M. Guermoui, K. Gairaa, J. Boland and T. Arrif.: 'A Novel Hybrid Model for Solar Radiation Forecasting Using Support Vector Machine and Bee Colony Optimization Algorithm: Review and Case Study', Journal of Solar Energy Engineering, vol. 143, No. 2, p. 020801, 2021.

[23] M. Colak, M. Yesilbudak and R. Bayindir.: 'Daily Photovoltaic Power Prediction Enhanced by Hybrid GWO-MLP, ALO-MLP and WOA-MLP Models Using Meteorological Information', Energies, Vol. 13, No. 4, p. 901, 2020.

[24] S.D. Sarkar and A.S. KB.: 'Face recognition using artificial neural network and feature extraction', In 2020 7th International Conference on Signal Processing and Integrated Networks (SPIN), IEEE, pp. 417-422, February 2020.

[25] S. Andayani, N.H.W. B.S. Marwoto and M.M.Hapsari.: 'Exploitation of Nasolabial Folds for Happy Smile Recognition on an Image Using ANN' In 7th International Conference on Research, Implementation, and Education of Mathematics and Sciences (ICRIEMS 2020), Atlantis Press, pp. 329-333, March 2021.

[26] P. Rama and S. Murugan.: 'Localization Approach for Tracking the Mobile Nodes Using FA Based ANN in Subterranean Wireless Sensor Networks', Neural Processing Letters, vol. 51, No. 2, pp.1145-1164, 2020.

[27] B. Madagouda and R. Sumathi.: 'Artificial Neural Network Approach using Mobile Agent for Localization in Wireless Sensor Networks', Advances in Science, Technology and Engineering Systems Journal,vol. 6, pp.1137-1144, 2021.

[28] M. Sajjad, Z.A. Khan, A. Ullah, T. Hussain, W. Ullah, M.Y. Lee and S.W. Baik, S. W.: 'A novel CNN-GRU-based hybrid approach for short-term residential load forecasting', IEEE Access, vol. 8, pp. 143759-143768, 2020.

[29] P. Kumari and D. Toshniwal, D.: 'Long short term memory–convolutional neural network based deep hybrid approach for solar irradiance forecasting', Applied Energy, vol. 295, p. 117061, 2021.

[30] F. Kaytez.: 'A hybrid approach based on autoregressive integrated moving average and least-square support vector machine for long-term forecasting of net electricity consumption', Energy, vol. 197, p. 117200, 2020.

[31] Z.F. Liu, S.F. Luo, M.L. Tseng, H.M. Liu, L. Li and A.H.M. Mashud.: 'Short-term photovoltaic power prediction on modal reconstruction: A novel hybrid model approach', Sustainable Energy Technologies and Assessments, vol. 45, p. 101048, 2021.

[32] X. Sui, S. He, S.B. Vilsen, J. Meng, R. Teodorescu and D. I. Stroe.: 'A review of non-probabilistic machine learning-based state of health estimation techniques for Lithium-ion battery', Applied Energy, vol. 300, p. 117346, 2021.

[33] X. Y. Chen and K.W. Chau.: 'Uncertainty analysis on hybrid double feedforward neural network model for sediment load estimation with LUBE method', Water Resources Management, vol. 33, No. 10, pp. 3563-3577, 2019.

[34] R. García-Ródenas, L.J. Linares and J.A. López-Gómez.: 'Memetic algorithms for training feedforward neural networks: an approach based on gravitational search algorithm. Neural Computing and Applications, vol. 33, No. 7, pp. 2561-2588, 2021.

[35] S.D. Al-Majidi, M.F. Abbod and H.S. Al-Raweshidy. : 'A particle swarm optimisation-trained feedforward neural network for predicting the maximum power point of a photovoltaic array', Engineering Applications of Artificial Intelligence, vol. 92, p. 103688, 2020.

[36] S.A. Abdulkarim and A.P. Engelbrecht.: 'Time series forecasting with feedforward neural networks trained using particle swarm optimizers for dynamic environments', Neural Computing and Applications, vol. 33, No. 7, pp. 2667-2683, 2021.

[37] T. Mahardhika.: 'Hybrid Algorithm as alternative method for optimization, a combination Genetic Algorithm and Particle Swarm Optimization' In Journal of Physics: Conference Series, vol 1764, No. 1, p. 012040, 2021.

[38] A. I. Nusaif and A. L. Mahmood.: 'MPPT Algorithms (PSO, FA, and MFA) for PV System Under Partial Shading Condition, Case Study: BTS in Algazalia, Baghdad', International Journal of Smart Grid-ijSmartGrid, vol. 4, No. 3, pp. 100-110, 2020.

[39] A.K. Pani and N. Nayak.: 'A Short Term Forecasting of PhotoVoltaic Power Generation Using Coupled Based Particle Swarm Optimization Pruned Extreme Learning Machine', International Journal of Renewable Energy Research (IJRER), vol. 9, No. 3, pp. 1190-1202, 2019.

[40] M.O. Okwu and L.K. Tartibu.: 'Particle Swarm Optimisation', In: Metaheuristic Optimization: Nature-Inspired Algorithms Swarm and Computational Intelligence, Theory and Applications. Studies in Computational Intelligence Springer Cham, vol. 927, pp 5-13, 2021.

[41] I.A. Samuel, T.M. Adeyemi-Kayode, A.A. Olajube, S.T. Oluwasijibomi and A.I. Aderibigbe.: 'Artificial Neural Network and Particle Swarm Optimization for Medium Term Electrical Load Forecasting in a Smart Campus', International Journal of Engineering Research and Technology, vol. 13, No. 6, pp. 1273-1282, 2020.

[42] Q.E. Abbas and S.B. Jang.: 'A Comparative Study of Machine Learning Algorithms Based on Tensorflow for Data Prediction', KIPS Transactions on Computer and Communication Systems, vol 10, No. 3, pp. 71-80, 2021.

[43] K. Wang, X. Qi, X and H. Liu.: 'A comparison of day-ahead photovoltaic power forecasting models based on deep learning neural network', Applied Energy, vol. 251, p. 113315, 2019.

[44] D. Lee and K. Kim.: 'PV power prediction in a peak zone using recurrent neural networks in the absence of future meteorological information', Renewable Energy, vol. 173, pp. 1098-1110, 2021.

[45] Y. Wang, A.W. Kandeal, A. Swidan, S.W. Sharshir, G.B. Abdelaziz, M.A. Halim, A.E. Kabeel and N. Yang.: 'Prediction of tubular solar still performance by machine learning integrated with Bayesian optimization algorithm', Applied Thermal Engineering, vol. 184, p. 116233, 2020.

[46] M.S. Alam, N. Sultana and S.Z. Hossain.: 'Bayesian optimization algorithm based support vector regression analysis for estimation of shear capacity of FRP reinforced

concrete members', Applied Soft Computing, vol. 105, p. 107281, 2021.

[47] W. Huang, X. Zhang and W. Zheng.: 'Resilient power network structure for stable operation of energy systems: A transfer learning approach', Applied Energy, vol. 296, p. 117065, 2021.

[48] A. Kulshrestha, V. Krishnaswamy and M. Sharma.: 'Bayesian BILSTM approach for tourism demand forecasting', Annals of tourism research, vol. 83, p. 102925, 2020.

[49] S. P.Durrani, S. Balluff, L. Wurzer and S. Krauter.: 'Photovoltaic yield prediction using an irradiance forecast model based on multiple neural networks', Journal of Modern Power Systems and Clean Energy, vol. 6, No. 2, pp. 255-267, 2018.

[50] F. Shahid, A. Zameer and M. Muneeb.: 'Predictions for COVID-19 with deep learning models of LSTM, GRU and Bi-LSTM', Chaos, Solitons & Fractals, vol. 140, p. 110212, 2020.

[51] D. Jia, J. Hua, L. Wang, Y. Guo, H.Guo, P. Wu, M. Liu and L. Yang.: 'Estimations of Global Horizontal Irradiance and Direct Normal Irradiance by Using Fengyun-4A Satellite Data in Northern China.', Remote Sensing, vol. 13, No. 4, p.790, 2021.

[52] I. M. Opedare, T. M., Adekoya and A. Longe.: 'Optimal Sizing of Hybrid Renewable Energy System for off-Grid Electrification: A Case Study of University of Ibadan Abdusalam Abubakar Post Graduate Hall of Residence', International Journal of Smart Grid-ijSmartGrid, vol. 4, No. 4, pp. 176-189, 2020.

[53] A. S. Alsagri, A. A. Alrobaian and M. Nejlaoui.: 'Techno-economic evaluation of an off-grid health clinic considering the current and future energy challenges: A rural case study', Renewable Energy, vol. 169, pp 34-52, 2021.

[54] J. Ramirez-Vergara and L. B. Bosman, W. D. Leon-Salas and E. Wollega.: 'Ambient temperature and solar irradiance forecasting prediction horizon sensitivity analysis', Machine Learning with Applications, vol. 6, p. 100128, 2021.

[55] M. B. Ammar, M. A. Zdiri and R. B. Ammar.: 'Fuzzy Logic Energy Management between Stand-alone PV Systems', International Journal of Renewable Energy Research (IJRER), Vol. 11, No. 3, pp. 1238-1249, 2021

[56] A. Y. Hatata, G. Osman and M. M. Aladl, .: 'An optimization method for sizing a solar/wind/battery hybrid power system based on the artificial immune system', Sustainable energy technologies assessments, vol. 27, pp. 83–93, 2018.

[57] H. M. Ridha, C. Gomes, H. Hizam, M. Ahmadipour, A. A. Heidari and H. Chen.: 'Multi-objective optimization and multi-criteria decision-making methods for optimal design of standalone photovoltaic system: A comprehensive review', Renewable and Sustainable Energy Reviews, vol. 135, p. 110202, 2021.

[58] M. Al-Gabalawy, N. S. Hosny, J. A. Dawson and A. I. Omar .: 'State of charge estimation of a Li-ion battery based on extended Kalman filtering and sensor bias', International Journal of Energy Research, vol. 45, No.5, pp. 6708-6726, 2021.

[59] O. B. H. B. Kechiche, M. Hamza and H. Sammouda.: 'Dimensioning of an Autonomous Photovoltaic Installation: Case Study in Msaken, Sousse (Tunisia) ', Energy Efficiency and Sustainable Lighting, p. 109, 2020.

[60] M. F. Ishraque, S. A. Shezan, S. J. N. Nur and M. S. Islam.: 'Optimal Sizing and Assessment of an Islanded Photovoltaic-Battery-Diesel Generator Microgrid Applicable to a Remote School of Bangladesh', Engineering Reports, vol. 3, No. 1, p. 12281, 2021.